An airway tree-shape model for geodesic airway branch labeling

Aasa Feragen[1], Pechin Lo[1], Vladlena Gorbunova[1], Mads Nielsen[1], Asger Dirksen[2], Joseph M. Reinhardt[3], Francois Lauze[1], Marleen de Bruijne[1] *

[1]Department of Computer Science, University of Copenhagen, Denmark
{aasa, marleen}@diku.dk
[2]Department of Orthopedics and Internal Medicine, University of Copenhagen, Denmark
[3]Department of Biomedical Engineering, University of Iowa, USA
http://image.diku.dk/aasa

Abstract. We present a mathematical airway tree-shape framework where airway trees are compared using geodesic distances. The framework consists of a rigorously defined shape space for treelike shapes, endowed with a metric such that the shape space is a geodesic metric space. This means that the distance between two tree-shapes can be realized as the length of the geodesic, or shortest deformation, connecting the two shapes. By computing geodesics between airway trees, as well as the corresponding airway deformation, we generate airway branch correspondences. Correspondences between an unlabeled airway tree and a set of labeled airway trees are combined with a voting scheme to perform automatic branch labeling of segmented airways from the challenging EXACT'09 test set. In spite of the varying quality of the data, we obtain robust labeling results.

Keywords: Airway branch registration, tree-shape model, airway shape model, tree metric, tree matching

1 Introduction

Medical imaging is an important diagnostic tool, and along with this tool comes a need for automatic analysis of medical images. Tree-structures are important in this context due to their roles as delivery systems for fluids and gases, which ties them directly and indirectly to a number of diseases. For instance, smoker's lung (COPD) is tied to properties of the airway, such as the airway wall thickness [11, 14].

In order to monitor progression of diseases and determine the range of normal variation in healthy anatomical trees, we need to compare measures between scans with varying characteristics. For instance, one needs to be able to compare measurements of airway dimensions, made at specified sites in the airway, between several patients. In this paper, we provide a robust way to make such comparisons for airway trees by giving anatomical labels to branches in the

* This work is partially funded by the Lundbeck Foundation.

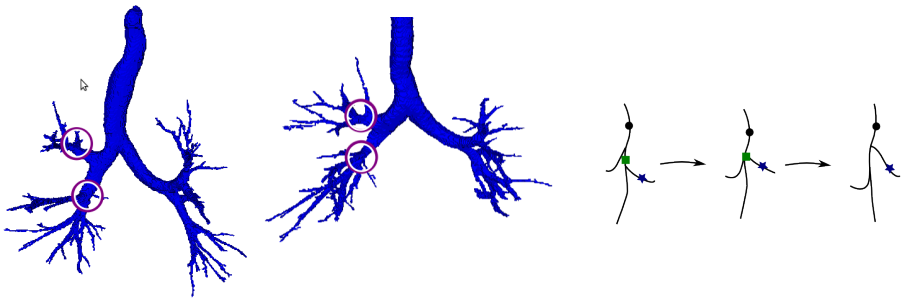

(a) (b) (c)

Fig. 1. ((a-b) Examples of segmented airways (CASE31 and CASE32 in the EXACT'09 dataset). The topological structures of the two trees are different, especially the circled "trifurcation-like" regions in the (image) left hand side, shown as trifurcations in fig. 3(a). c) By tracing points (illustrated by the circle, square and star) through the geodesic deformation between two tree-shapes, we obtain a registration of points and branches of the two endpoint tree-shapes. Branches which are collapsed during the tree deformation, are not traced further, as illustrated by the square.

airway based on the shape of the airway centerline tree. The technique uses a model of airway tree-shape which incorporates two notions: tree topology (i.e., parent/child connectivity) and geometry, defined by branch shapes (e.g., through landmark points).

Branch matching is, indeed, both a tree-topological and a geometric problem. Topological differences are particularly problematic for comparison and matching of anatomical trees such as the airways. These differences can come from noise in terms of spurious or missing branches, due to problems in the image recording and processing procedures. Topological differences can also come from anatomical variation between different patients, see figs. 1(a) and 1(b). Most current anatomical tree labeling methods focus, however, *either* on branch geometry *or* on tree topology. In this article we perform matching based on geodesics in an airway tree-space based on the tree-shape framework developed by Feragen et al. [3], where a varying tree topology becomes an integral part of the shape geometry. Not only is this framework geometrically very natural; it also handles tree-topological differences in a continuous, morphological way.

The airway tree model proposed in this paper consists of a shape space construction for treelike shapes, endowed with a geodesic metric. Any two treelike shapes are connected by a shortest possible deformation, or tree-space path (geodesic), whose length defines a distance between the shapes. Throughout the deformation, the initial tree changes its tree-topological structure to obtain an optimal match with the second tree. This makes the tree-shape framework well suited for branch registration in both inter- and intra-patient pairs of airways. The deformation, which is unique for sufficiently local data, induces a matching of points along the tree-shape branches as illustrated in fig. 1(c). In a leave-one-out fashion, we generate automatic branch labels on any given airway tree by

matching it with the other airway trees, which have been manually labeled by an expert. The geodesic matching is combined with a branchwise vote among anatomical labels induced by the matches, giving a robust automatic branch labeling.

The main contributions of this paper are i) the adaptation of the tree-shape framework of [3] to airway trees, giving a new version of the shape space; ii) a thorough explanation of the underlying geometric ideas, making the tree-shape model available for a broader community; iii) turning the computed geodesics into an actual branch matching; and iv) the fusion of several branch matchings through a voting scheme in order to obtain branch labelings.

The airway shape model has potential for applications beyond branch matching and labeling. Labels or geodesic distances could be used to classify airways into shape- and structure-dependent phenotypes, and the shape space framework also opens for defining new biomarkers based on the whole airway shape – topology and geometry combined. Moreover, the shape space framework used here is very general, and can be transferred to other types of data, e.g., vascular trees or medial axes, with little effort.

1.1 Related work.

Registration, branch matching and branch labeling in anatomical trees have been studied in various ways for the past decade. Some of the most successful methods are based on using association graphs [5,9,12]. Given two initial trees or graphs, their association graph is a larger graph, which contains information from both initial graphs. Branch matchings are induced by maximal cliques in the association graph. The association graph and its maximal clique are predominantly combinatorial constructions, although they can depend on geometric properties of the initial trees. Separating the analysis of geometric and combinatorial properties like this is somewhat artificial, as the geometric and topological structures play together in defining the efficiency of an anatomical tree as a space-filling structure [8,15]. Moreover, finding the maximal clique is NP hard, making exact computation intractable.

A more basic labeling method is given by van Ginneken et al. [13], where an airway tree branch labeling is made recursively, starting at the trachea, as part of the segmentation process. Labels are assigned using measures such as radius, orientation and bifurcation angle. Such a labeling approach is likely to be vulnerable to differences in topological structure, as is also noted by the authors. A different approach is that of Kaftan et al. [4], who match tree *paths* rather than branches. They avoid the difficulty with different tree-topological structures, but also lose all information stored in the topological structure. Their model does not seem to have applications beyond matching, and in particular does not generate branch labels. Smeets et al. [10] match branches from lung vessel trees using pairwise distances between nodes both in 3D Euclidean space and along the tree to generate distance matrix "fingerprints", which are matched in order to generate a matching. Bülow et al. [2] match airway tree branches without connectivity information, using only branch shape.

These methods all focus on one out of two properties of a tree-shape: tree topology [5, 9, 12], or branch-wise geometry [2, 4, 10]. However, the airway tree is *both* topology and branch geometry. This duality is precisely what makes matching and labeling difficult. Our airway tree-shape model is ideal for modeling airway trees because it considers topology and geometry simultaneously.

The rest of the paper is organized as follows: The airway tree-shape model and the tree-shape metric are presented in sec. 2; experimental details and results are presented in sec. 3, which are discussed in sec. 4 and concluded in sec. 5.

2 The tree-shape space

The proposed method uses airway centerlines as input. Each branch centerline is associated with an edge in a combinatorial airway tree, endowed with a hierarchical tree structure (parent/child) which describes branch connectivity. Shape information is represented by edgewise attributes, in this case a fixed number of equally spaced landmark points along each branch centerline (the equal spacing length varies from branch to branch).

We build a space of airway tree-shapes based on the tree-shape model defined by Feragen et al. [3]. Any tree-shape, such as an airway tree-shape, is represented as a pair (T, f) of a combinatorial tree-structure T with edgewise shape attributes f, see fig. 2. Here $T = (V, E, r)$ is a tree with vertices V, edges $E \subset V \times V$, and a root r. The shape attributes given by n landmark points per edge are specified by a function $f\colon E \to \mathbb{R}^{3n}$.

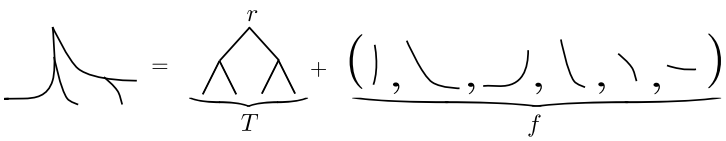

Fig. 2. A tree-shape is represented mathematically as a pair (T, f) where T is a binary, combinatorial tree and $f : E \to \mathbb{R}^{3n}$ assigns a shape-descriptor from $\mathbb{R}^{3n}$ to each edge.

2.1 Intuitive description of a geodesic tree-shape space

Our goal is to construct a continuous space of deformable trees, and this goal poses some constraints on the possible geometric structure of the space of tree-like shapes. To see this, first consider airway trees with a single fixed topological structure $T = (V, E, r)$. All such trees are described by a point in the same Euclidean product space $\prod_E \mathbb{R}^{3n}$. Next, divide the set of all airway trees into classes with fixed topological structure. Each airway tree class lives within its own Euclidean space $\prod_{E_i} \mathbb{R}^{3n}$, and the space of all airway tree-shapes is a disjoint union $X = \bigsqcup \left(\prod_{E_i} \mathbb{R}^{3n}\right)$ of shape spaces, one for each topological structure. We consider each $\prod_{E_i} \mathbb{R}^{3n}$ as a component of the larger space of all airway tree-shapes.

We should tie these components together into a large shape space that connects all airway trees. In order to understand how to tie the components together, we consider how the tree-topological structure changes throughout deformations.

For example, in fig. 3(a), the LMB branch is shown as the parent of a trifurcation, with the LUL, LLB6 and LB6 branches emanating from it. In reality, one will not find a trifurcation, but a pair of bifurcations, e.g., as seen in the two airway subtrees $\mathcal{T}_1$ and $\mathcal{T}_2$ in fig. 3(b). A geodesic deformation from $\mathcal{T}_1$ to $\mathcal{T}_2$ should interchange the order of the LUL and LB6 branches by passing through a tree of the type $\mathcal{T}$ shown in fig. 3(b). This tree can be obtained as a limit of a sequence of trees with a fixed structure. For instance, such a sequence can start at $\mathcal{T}_1$ or $\mathcal{T}_2$ and successively shrink the small branch until collapsing onto one of the representations of $\mathcal{T}$. Similar sequences can be found for many different topological structures, represented by tree-shapes $\mathcal{T}_i$, where slowly deleting certain edges in $\mathcal{T}_i$ converges towards a tree of type $\mathcal{T}$. By following sequences within different components of the tree-space, where all the tree-shapes in the i^{th} component have the same structure as $\mathcal{T}_i$, we reach the same tree-shape $\mathcal{T}$. This must mean that in order to have a tree-space where the trees can continuously deform from one topological structure to another, as in fig. 3(b), the tree-space components of the $\mathcal{T}_i$ must all intersect along the component of $\mathcal{T}$. In the next section, we shall see how such a tree-space can be defined mathematically.

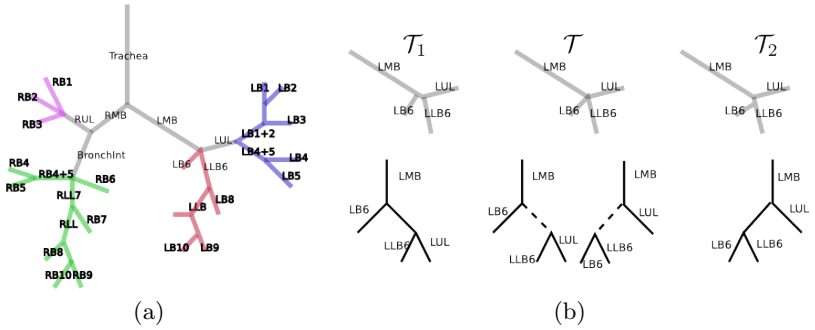

Fig. 3. (a) This figure is best viewed in color. In the first generations of the airways, the branching structure is fairly pre-determined due to anatomy, and the branches have names. (b) The tree-shape $\mathcal{T}$ can be obtained as a limit of a sequence where a branch is disappearing – for instance, $\mathcal{T}$ can be obtained by shrinking a branch in either $\mathcal{T}_1$ or $\mathcal{T}_2$, or a number of other tree-shapes $\mathcal{T}_i$. This illustrates how trifurcations can be interpreted as pairs of bifurcations; their combinatorial representations are shown in the bottom row. This causes some problems in the representation space X defined in sec. 2.2, since, for instance, the path from $\mathcal{T}_1$ to $\mathcal{T}$ to $\mathcal{T}_2$ is impossible in X. Passing from $\mathcal{T}_1$ or $\mathcal{T}_2$ to $\mathcal{T}$ is easy, but the two representations of $\mathcal{T}$ correspond to different points in X, and the path $\mathcal{T}_1 \to \mathcal{T} \to \mathcal{T}_2$ is not possible in X. This path is, however, possible in the quotient space $\bar{X}$, where different representations of the same tree are glued together in one point. We define $\bar{X}$ to be the space of treelike shapes.

2.2 Mathematical definition of the tree-shape space

Having established an intuitive understanding of the geometry of the tree-space, we shall give a more concrete definition. Recall that any tree-shape is represented by a pair (T, f) consisting of a combinatorial tree T and edge shape attributes f. In order to study trees of different sizes and topologies in one unified setting, all shapes are represented by a fixed combinatorial tree $T = (V, E, r)$, which is *large enough*; e.g., if all the tree-shapes have depth N, then T could be the full binary tree of depth N. Smaller trees are represented in the tree-space by endowing extra edges with zero attributes, see fig. 3(b). All trees are represented by a point in the Euclidean representation space

$$X = \prod_{e \in E} \mathbb{R}^{3n}. \tag{1}$$

Assume, moreover, that T is binary. All non-binary tree-shapes can be represented using a binary combinatorial tree by collapsing internal branches, as described in fig. 4. The space $X = \prod_{e \in E} \mathbb{R}^{3n}$ contains every tree-shape represented at least once. Some tree-shapes are even represented at several points in X, and as a consequence, some natural tree-shape deformations cannot be represented as paths in X, see fig. 3(b). This problem is solved by generating an equivalence relation $\sim$ on X where different representations of the same shape are identified; now the space of tree-shapes is defined as the quotient space $\bar{X} = X/\sim$.

Definition 1. *We say that two representations in X define the "same tree-shape" when the following holds: Starting with the two tree-shape representatives $x_1 = (T, f_1)$ and $x_2 = (T, f_2)$, remove all branches with zero attribute, and consider the resulting (possibly no longer binary) tree-shape representations $(T_1, \tilde{f}_1)$ and $(T_2, \tilde{f}_2)$. Here, T_1 and T_2 are ordered, combinatorial, rooted trees. If, up to a topology-preserving reordering of the branches, these two attributed trees are exactly the same, then the tree-shapes are the same and the two representations are defined to be* equivalent. *We write $x_1 \sim x_2$.*

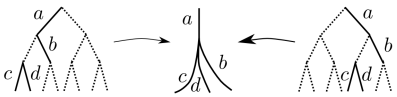

Fig. 4. Trees which are *not* binary, or which are smaller than T, are represented by cancelling extra edges, endowing them with the attribute zero (dotted lines). This leads to several representations of the same tree-shape. By identifying those different representations that represent the same shape, we construct our shape space as the quotient space $\bar{X}$.

All equivalent points are identified by forming the *quotient space* $\bar{X}$ of the equivalence relation [1], that is:

$$\bar{X} = X/\sim = \{\bar{x} | x \in X\}, \tag{2}$$

where

$$\bar{x} = \{z \in X | z \sim x\}. \tag{3}$$

The points in $\bar{X}$ are equivalence classes $\bar{x}$ in X – by abuse of notation we use $\bar{x}$ to denote both points in $\bar{X}$ and subsets of X. Geometrically, this construction corresponds to gluing together those points in the representation space X that represent the same tree-shape. As most of the points only have one representative, this creates a new space $\bar{X}$ with self intersections at points with several representatives. Many geometric properties of X are inherited by $\bar{X}$. The quotient space $\bar{X}$ is the space of treelike shapes.

2.3 Metrics on the shape space

The Euclidean metric on X induces a standard *quotient metric* d on $\bar{X}$ [1], called Quotient Euclidean Distance (QED), defined as follows:

$$d(\bar{x}, \bar{y}) = \inf_{k \in \mathbb{N}} \left\{ \sum_{i=1}^{k} \|a_i - b_i\| : a_1 \in \bar{x}, b_i \text{ equivalent to } a_{i+1}, b_k \in \bar{y} \right\}. \tag{4}$$

Here, the norm $\|\cdot\|$ denotes the Euclidean norm on X, and $\bar{x}$ is the equivalence class of the point $x \in X$. Thus, when we write $a_1 \in \bar{x}$, this means that a_1 is a point belonging to the equivalence class $\bar{x}$ as a subset of X, or equivalently, $a_1 \sim x$.

One interpretation of eq. 4 is that a QED geodesic consists of a sequence of k Euclidean lines, which are cut and concatenated whenever the geodesic deformation switches between two representations b_i and a_{i+1} of the same tree. Typically, these identified points correspond to internal topological transitions in the tree-shape structure. The infimum is taken over all possible concatenations of lines for any k. E.g., the geodesic from $\mathcal{T}_1$ to $\mathcal{T}_2$ in fig. 3(b) consists of the Euclidean line from $\mathcal{T}_1$ to the first representative of $\mathcal{T}$, concatenated with the Euclidean line from the second representative of $\mathcal{T}$, to $\mathcal{T}_2$.

The QED metric is locally very well-behaved. In particular, geodesics between data points and various forms of average shapes will exist and be unique [3]. This makes the tree-shape space and its geodesic deformations well suited for registration. The tree-space construction described above is completely general, and applies to any trees with continuous edge attributes, not only shapes.

2.4 Airway tree-shape space

In order to compute the geodesic connecting two $3D$ tree-shapes such as airways, we consider all possible branch orders on the trees in order to find an optimal branch alignment. The number of possible orders grows exponentially with the size of the trees, resulting in computational difficulties. In the case of airway trees, however, some branches are easy to identify, e.g., the main bronchi and some of the lobar bronchi seen in fig. 3(a). We significantly reduce computational complexity by identifying and fixing the branches $E_{\text{fixed}} =$

{RMB, LMB, RUL, BronchInt, LB6, LLB6, LUL}, which are present and easy to identify in most data trees. In this way, we consider topological variation only in the lobar subtrees T_{RUL}, T_{LUL}, $T_{\mathrm{BronchInt}}$, T_{LLB6}, T_{LB6} following these, shown in colors in fig. 3(a). The airway shape space is then

$$\left(\prod_{e\in E_{\mathrm{fixed}}} \mathbb{R}^{3n}\right) \oplus \overline{\left(\prod_{e\in E_{\mathrm{RUL}}} \mathbb{R}^{3n}\right)} \oplus \cdots \oplus \overline{\left(\prod_{e\in E_{\mathrm{LLB6}}} \mathbb{R}^{3n},\right)} \tag{5}$$

where the first component is Euclidean and the others are quotient spaces. The symbol $\oplus$ denotes direct sum, or Cartesian product.

2.5 Computing geodesics

Computing the geodesics from eq. 4 is generally NP hard. The number k of Euclidean concatenations that need to be checked will, in practice, be bounded for any given pair of trees, but it will grow exponentially with the number of edges in the trees. We make an approximation by bounding k in eq. 4 for each lobar subtree. That is, we fix some number $K \in \mathbb{N}$, and approximate the distance in eq. 4 by computing

$$d(\bar{x},\bar{y}) = \inf_{k\leq K} \left\{ \sum_{i=1}^{k} \|a_i - b_i\| : a_1 \in \bar{x}, b_i \text{ equivalent to } a_{i+1}, b_k \in \bar{y} \right\}. \tag{6}$$

This corresponds to assuming that the tree-shape represented throughout geodesic will undergo at most K internal topological changes. In order to compute the approximated distance, a naive implementation is to list all the allowed combinations of topological changes, to compute the shortest version of a path going through each of those particular changes, and choose the shortest among the resulting paths. This is equivalent to Algorithm 1 from [3].

2.6 Branch label extraction

Using a geodesic deformation from a labeled airway tree to an unlabeled one, as seen in fig. 1(c), labels from a labeled tree can be propagated to the branches of an unlabeled tree.

For data with large variation in topology, we would normally need to choose a rather high bound K on k in eq. 6, in order to obtain the true geodesics between data points. This is punished by a large increase in computation time. We avoid this problem by matching with multiple labeled trees, and thus extracting a number of candidate labels for each branch. This is followed by a voting scheme, where nearby trees, for which the approximation is good, are expected to win the vote. Given a training set of airway trees with manually assigned labels, a new airway tree is first matched with all the trees in the training set, and sets of labels are propagated to the branches of the unlabeled tree. Each branch is assigned a pool of labels, among which the majority vote is selected as a new, automatically extracted branch label.

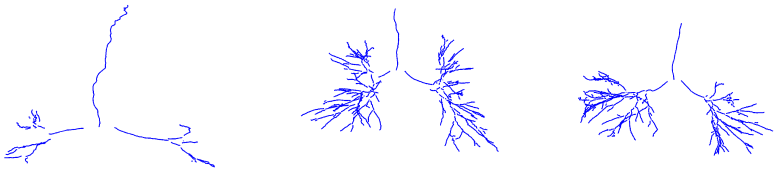

Fig. 5. The centerline trees of CASE26, CASE34 and CASE39, respectively. Note the large variation in size and topological structure; in particular CASE39 is missing the upper lobar trees.

3 Experimental validation

Experiments were made on airways from the EXACT'09 challenge test set [7], consisting of 20 CT scans from 15 different subjects, labeled as CASE21 - CASE40. The EXACT'09 challenge was a segmentation competition, and the CT scans come from a wide range of sources, states of breathing, and are processed using different methods [7]. As a result, the segmented airway trees display great variation in size, shape and noise level.

The airway trees were segmented from the CT scans using a voxel classification based airway tree segmentation algorithm by Lo et al. [6]. The centerlines were extracted from the segmented airway trees using a modified fast marching algorithm, directly giving a tree structure. Due to the segmentation method, the centerline trees are not connected, but have gaps at each bifurcation, as seen in fig. 5. This is not a problem, as the proposed matching method relies on the edge shapes, which are sufficiently well described in the disconnected model, along with parent/child connectivity information.

Leaves with segmented volume less than 10 mm^3 were assumed to be noise and pruned away, and the centerlines were sampled with 6 equidistant landmark points along each edge. For each edge, the landmark points were translated so that the first landmark point was aligned with the origin. In this way, large differences in edges of low generation do not affect the whole subtree following them. To account for variation in size, each airway tree was normalized by the constant scaling factor 1/length(LMB), chosen since the LMB branch is present and easy to measure in all segmentations. The trachea was left out in the experiment due to varying cut-off points. The next few branches (RMB, LMB, RUL, BronchInt, LB6, LLB6, LUL) were detected based on the orientation and extent of their subtrees. Branches from the first $6-7$ generations were matched, whenever they were present in the segmentation.

3.1 Branch labeling

Each airway tree was aligned with all other airway trees in the dataset through computing geodesics with $K = 2$ for each lobar subtree (that is, permitting one

CASE	21	22	23	24	25	26	27	28	29	30
% correct	75	88.2	92.9	80	77.8	86.7	88.9	94.4	66.7	89.5
# correct	12	15	13	12	14	13	16	17	14	17
CASE	31	32	33	34	35	36	37	38	39	40
% correct	90	76.5	88.9	100	83.3	78.9	66.7	80	30	76.5
# correct	18	13	16	13	15	15	12	8	4	13

Table 1. Results from the branch labeling; the percentage of correctly labeled branches among all branches labeled by the algorithm, and the number of branches correctly labeled by the algorithm. CASE39 is an outlier: both upper lobes were missing from the segmentation, making the algorithm fail. When the outlier is left out, we correctly label 83% of the branches on average.

structural transition in each of the five lobar subtrees). When computing the distances, not only the length of the geodesic from one tree to another, but also the geodesic from the first tree to the second were recorded. Using the geodesic we obtained a branch-wise matching by recording which edges are mapped onto which.

The reference airway trees from EXACT'09 were labeled manually by a trained image analyst. Up to 34 labels were assigned according to a standard nomenclature used in bronchoscopy. All cases were reviewed by a pulmonologist after labeling. For each pair of airway trees, a ground truth branch matching was induced from the anatomical labels. Several branches found by the registration were not labeled by the human experts, and were left out in evaluation.

The voting scheme was made based on the 20-airway dataset in a leave-one-out fashion, where each airway tree was matched with the remaining 19 and given a branch labeling based on the majority vote. In this way, labels down to the sixth generation of each airway tree were computed using the rest of the airway trees as training set. The best label for any given branch was obtained by voting among the labels. Branch labels with less than 55% voting consensus or less than 4 votes in total were discarded. The results are found in table 1; the overall success rate is 83%. We can obtain better scores by insisting on a higher majority vote; however, this implies labeling fewer branches.

4 Discussion

Tschirren et al. [12], van Ginneken et al. [13] and Bülow et al. [2] performed labeling on airway trees with success rates of 97%, 90% and 69%/40% (using different features), respectively. Our success rate is 83%, which – taking the level of variation in the dataset into account – is high. Since the datasets used are all different, a direct comparison of percentages is not possible.

The large variance in our results is natural since the EXACT'09 data come from a wide range of sources, and are made with different subjects, scanners, scan- and reconstruction protocols etc, as described in [7, table 1]. This poses

a great challenge: the structural differences between the segmented airway trees are very large, as illustrated in figs. 5 and 6, and the amount of noise is very different from tree to tree. We might have dealt with this problem by making a better approximation of the QED metric. Instead, based on the hypothesis that trees which are close together will be topologically similar, we choose to use a coarse but efficient approximation combined with a voting scheme.

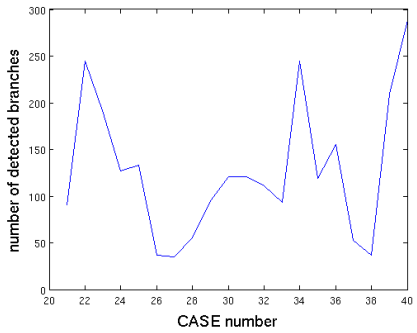

Fig. 6. The number of detected branches in the EXACT'09 airway trees is very variable. Note also that this number is affected by the level of structural noise, and might not directly correspond to the number of anatomical branches.

5 Conclusion

Based on a geometric model for shapes with a treelike structure, we have developed a technique for automatic inter- and intra-patient registration of airway tree centerlines. The method has been evaluated by performing an airway branch labeling on the EXACT'09 dataset. In spite of the variation in the dataset, our labeling results are good, illustrating the potential of the shape framework.

The shape space framework is very general, and the tree-space can be enriched with additional attributes if wanted. There are very few airway and vessel tree labeling algorithms available, most of which are ad hoc, specialized heuristics. In contrast, our proposed method takes a principled approach, which is easy to generalize to other biological tree-structures, e.g.,vascular structures. This makes the proposed method both novel and important.

The airway shape model has potential for many applications beyond branch matching and labeling. The shape space has good properties for statistical analysis such as computation of means and modes of variation. Geodesic distances could be used to classify airways into shape- and structure-dependent phenotypes, and the shape space framework also opens for defining new imaging biomarkers based on the whole airway shape – topology and geometry combined. These extensions are, however, by no means straightforward, as we are

working in the non-smooth domain of tree-shape space. Further development of the shape space, numerical methods for tree-shape computations, and their applications are all topics of future work.

References

1. M. R. Bridson and A. Haefliger. *Metric spaces of non-positive curvature*. Springer-Verlag, 1999.
2. T. Bülow, C. Lorenz, R. Wiemker, and J. Honko. Point based methods for automatic bronchial tree matching and labeling. In *SPIE Med. Im.*, volume 6143, pages 225–234, 2006.
3. A. Feragen, F. Lauze, P. Lo, M. de Bruijne, and M. Nielsen. Geometries in spaces of treelike shapes. In *ACCV*, pages 671–684, 2010.
4. J.N. Kaftan, A.P. Kiraly, D.P. Naidich, and C.L. Novak. A novel multi-purpose tree and path matching algorithm with application to airway trees. In *SPIE Med. Im.*, volume 6143, pages 215–224, 2006.
5. H. Kitaoka, Y. Park, J. Tschirren, J. M. Reinhardt, M. Sonka, G. McLennan, and E. A. Hoffman. Automated nomenclature labeling of the bronchial tree in 3D-CT lung images. In *MICCAI (2)*, pages 1–11, 2002.
6. P. Lo, J. Sporring, H. Ashraf, J.J.H. Pedersen, and M. de Bruijne. Vessel-guided airway tree segmentation: A voxel classification approach. *Medical Image Analysis*, 14(4):527–538, 2010.
7. P. Lo, B. van Ginneken, J.M. Reinhardt, and M. de Bruijne. Extraction of Airways from CT (EXACT09). In *The 2nd Intl WS Pulm. Im. Anal.*, pages 175–189, 2009.
8. B. Mauroy, M. Filoche, E. R. Weibel, and B. Sapoval. An optimal bronchial tree may be dangerous. *Nature*, 427:633–636, 2004.
9. J. H. Metzen, T. Kröger, A. Schenk, S. Zidowitz, H-O. Peitgen, and X. Jiang. Matching of anatomical tree structures for registration of medical images. *Im. Vis. Comp.*, 27:923–933, 2009.
10. D. Smeets, P. Bruyninckx, J. Keustermans, D. Vandermeulen, and P. Suetens. Robust matching of 3d lung vessel trees. In *MICCAI 2010, Proc 3rd Intl WS Pulm. Im. Anal.*, pages 61–70, 2010.
11. L. Sørensen, P. Lo, A. Dirksen, J. Petersen, and M. de Bruijne. Dissimilarity-based classification of anatomical tree structures. In *Information Processing in Medical Imaging*, LNCS, 2011.
12. J. Tschirren, G. McLennan, K. Palágyi, E. A. Hoffman, and M. Sonka. Matching and anatomical labeling of human airway tree. *IEEE TMI*, 24(12):1540–1547, 2005.
13. B. van Ginneken, W. Baggerman, and E. van Rikxoort. Robust segmentation and anatomical labeling of the airway tree from thoracic CT scans. In *MICCAI 2008*, pages 219–226, 2008.
14. G. R. Washko, T. Dransfield, R. S. J. Estepar, A. Diaz, S. Matsuoka, T. Yamashiro, H. Hatabu, E. K. Silverman, W. C. Bailey, and J. J. Reilly. Airway wall attenuation: a biomarker of airway disease in subjects with COPD. *J Appl Physiol*, 107(1):185–191, 2009.
15. E. R. Weibel. What makes a good lung? *Swiss Med. Weekly*, (139(27-28)):375–386, 2009.